PRESSURE GRADIENT PARAMETER FOR OUTER LAYER SIMILARITY IN NONEQUILIBRIUM ADVERSE PRESSURE GRADIENT BOUNDARY LAYERS

Ralph J. Volino
Department of Mechanical and Nuclear Engineering
United States Naval Academy
Annapolis, Maryland, 21402, USA
volino@usna.edu

Michael P. Schultz
Department of Naval Architecture and Ocean Engineering
United States Naval Academy
Annapolis, Maryland, 21402, USA
mschultz@usna.edu

ABSTRACT

An effective pressure gradient parameter is proposed to capture upstream history effects in boundary layers subject to changing pressure gradients. The parameter is based on the assumption of an exponential decay of the local effective value of the parameter toward the local Clauser pressure gradient parameter, β, at any streamwise location. The parameter was tested using data sets from three studies in the literature. It proved effective for collapsing profiles of the mean velocity and Reynolds shear stress in cases with mild to moderate adverse pressure gradients with both increasing and decreasing β. In cases from another study with stronger pressure gradients and stronger departures from equilibrium, the new parameter was not as successful in collapsing the results. The parameter appears to be useful in some cases, but may need more development and modification to be more generally applicable.

INTRODUCTION

Canonical zero pressure gradient (ZPG) turbulent boundary layers on smooth flat walls approach an equilibrium state in which profiles of the mean velocity and turbulence quantities achieve approximate outer layer similarity when normalized using the boundary layer thickness, δ, and either the freestream velocity, U_e, or the friction velocity, u_τ. Under nonzero pressure gradients, similarity is possible if the Clauser pressure gradient parameter, $\beta=(\delta^*/\rho u_\tau^2)(dP/dx)$, is constant, where δ^* is the displacement thickness, ρ is density, P is pressure, and x is the streamwise coordinate. The equilibrium profiles depend strongly on the value of β, particularly for adverse pressure gradients (APG).

In many flows of practical interest, the pressure gradient and β are continuously changing, resulting in nonequilibrium conditions and profiles that change in the streamwise direction. Studies such as Bobke et al. (2017) have shown that profiles from nonequilibrium boundary layers with the same local β do not always agree, indicating a dependence on upstream history. Volino and Schultz (2026) showed that if the rate of change of β is sufficiently low, the boundary layer can remain in a state that is near equilibrium. The streamwise rate of change of β was quantified using a dimensionless streamwise coordinate proposed by Devenport and Lowe (2022), $(xu_\tau^2)/(\theta U_e^2)$, where θ is the momentum thickness. A physical argument for this streamwise scaling was given based on the turbulent mixing in the boundary layer and the large eddy turnover distance.

Several studies have considered effective β parameters for nonequilibrium boundary layers. The objective of an effective β is to account for upstream history effects. Vinuesa et al. (2017), for example, found an average β by integrating β as a function of momentum thickness Reynolds number from the start of an APG to a downstream point of interest. Gomez and McKeon (2025) proposed an average β found by integrating β as a function of streamwise location. Virgilio et al. (2025) also integrated over streamwise location and used an optimization to determine the length of the upstream region used in the averaging. Preskett et al. (2025) used a linear weighting in their averaging to give more emphasis to locations closer to the point in question and less to locations farther upstream. Mahajan et al. (2026) used a streamwise average of the parameter $\beta_{ZS}=(\delta/\delta)^3(u_\tau/U_e)^2\beta$ proposed by Maciel et al. (2018).

The various methods in the literature produce different results, and none appears to be universally useful for producing a parameter that results in similarity when comparing different flows. Questions for all methods involve determining how much of the upstream history to include for determining the behavior at a given location, how the behavior at upstream locations should be weighted depending on the distance upstream, and how these distances and weights may depend on the conditions of a particular flow and the type of pressure gradient (e.g. increasing or decreasing β).

The present paper proposes a new effective β that is based on an exponential decay toward the local β value at a given location. The method is described next, and then tested using data from the literature. It is applied to cases with both increasing and decreasing β, and used to compare mean velocity and Reynolds stress profiles.

PROPOSED EFFECTIVE β

The proposed effective β parameter, denoted β_e, is based on the hypothesis if β were constant downstream of a given location, then β_e should asymptotically approach the constant β value. An exponential decay is proposed, such that

$$\beta_e = \beta + (\beta_{eo} - \beta)e^{-a(x'-x'_o)} \quad (1)$$

where x' is a dimensionless streamwise distance, the subscript o indicates that value of β_e or x' at an upstream location, and a

is an empirical constant. The dimensionless distances proposed by Devenport and Lowe (2022)

$$x' = \frac{x u_{\tau o}^2}{\theta U_e^2} \quad (2)$$

is used. Alternative definitions using δ and δ^* in place of θ were also considered, but θ was found to produce better results, possibly because δ and δ^* tend to increase rapidly in an APG, which may give a false indication of the effective change in the large eddy turnover distance, while θ tends to change more slowly. As explained in Volino and Schultz (2026), the friction velocity, $u_{\tau o}$, is taken at the beginning of the APG region, while local values are used for U_e and θ. The friction velocity in Eq. (2) is intended to capture the effect of the Reynolds shear stress (turbulent mixing) in the boundary layer, which in a ZPG scales with u_τ^2. In an APG, however, the dimensional Reynolds shear stress does not drop with u_τ^2, so the upstream value is used in Eq. (2).

For a step change from an equilibrium condition with constant β to a different constant β, Eq. (1) is evaluated using β_{eo} as the upstream equilibrium value, β as the downstream value, and β_e as the local value changing over the distance x'-x'_o. For a continuously changing β, Eq. (1) is evaluated in incremental steps over distances $\Delta x'$, where β_{eo} is taken as the effective value at the end of the previous step, β is the local value at the end of the current step, and β_e is the predicted effective value at the end of the current step.

DATA SOURCES

Three sources of data were considered. The first includes five large eddy simulations (LES) from Bobke et al. (2017). The β distributions for these cases are shown in Fig. 1a. In two of these cases, β was approximately constant over most of the domain. In the other cases, β increased and then decreased, with a high value of about 4.5 in one case.

The second source of data is from the direct numerical simulations (DNS) of Gungor et al. (2016, 2022, 2024), with β distributions shown in Fig. 1b. In two of the cases, β rose continuously to much higher values (83 and 67) than in the Bobke et al. (2017) study, causing the boundary layer to approach separation. In the third case, β rose to about 33 before dropping to zero.

The third source of data is from the experimental results of Volino and Schultz (2026), shown in Fig. 1c. In these cases, the flows over smooth and rough flat walls in a recirculating water tunnel were studied. Local β values were as high as 11 and 200 on the smooth and rough walls, respectively. In cases 1-10 of this study, an APG region was directly downstream of a canonical ZPG region. In cases 11-13, an APG region was directly downstream of a favorable pressure gradient (FPG) region. In cases 14-15, there was an APG with an FPG directly upstream and a ZPG directly downstream. The change from an APG to a ZPG caused a significant departure from equilibrium.

The discussion below begins with the LES cases of Bobke et al. (2017) and presents results to show that matching β does not result in similarity in all cases, but the effective β_e of Eq. (1) produces better collapse. The cases of Gungor et al. (2016, 2022, 2024) and Volino and Schultz (2026) are then considered.

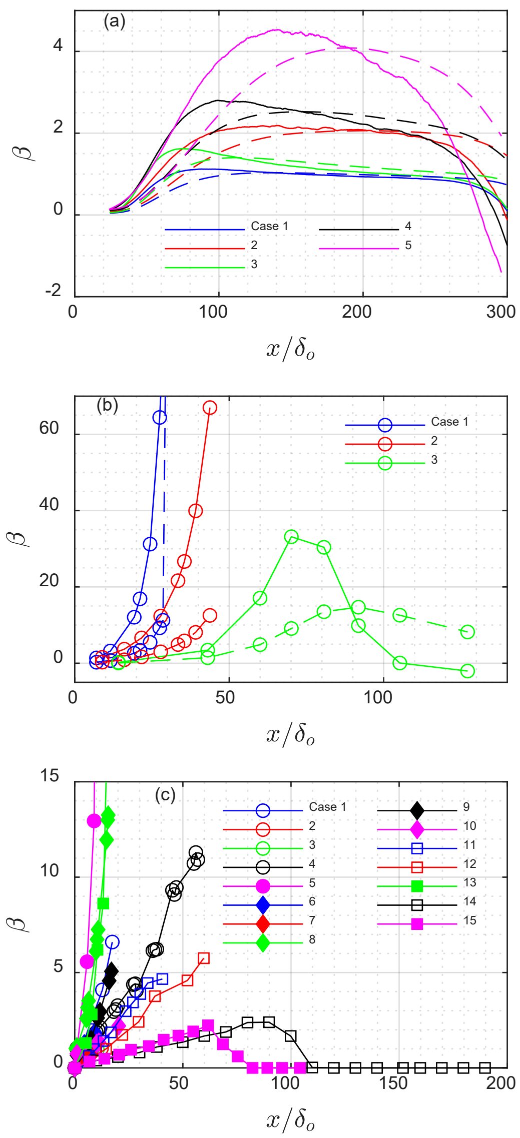

Figure 1. β (solid lines) and β_e (dashed lines) as a function of streamwise location normalized on upstream boundary layer thickness; a) Bobke et al. (2017), b) Gungor et al. (2016, 2022, 2024), c) Volino and Schultz (2026). For c), open symbols for smooth wall cases, filled symbols for rough wall cases.

RESULTS

One means of assessing equilibrium is through the relationship between β and the Clauser shape factor, $G = (U_e/u_\tau)(H-1)/H$, where $H = \delta^*/\theta$ is the shape factor. Results from the Bobke et al. (2017) cases are shown in Fig. 2 along with an equilibrium curve from Mellor and Gibson (1966). All of the cases shown exhibit significant departure from the equilibrium curve. In the region of increasing β, G at first does not rise as rapidly as the equilibrium curve would predict, but then overshoots the equilibrium curve while β is still rising. The overshoot suggests that the assumption made above that equilibrium would be approached asymptotically, may not be true in all cases. The difference from equilibrium is even more apparent in the regions of decreasing β, where the G values lie above the equilibrium curve and do not drop as fast as equilibrium would predict.

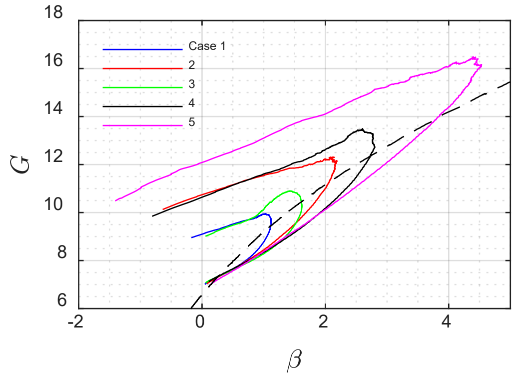

Figure 2. Clauser shape factor as a function of β for cases of Bobke et al. (2017). Dashed line is Mellor & Gibson (1966) equilibrium.

To illustrate the lack of similarity at a particular β, Fig. 3 shows profiles of the mean streamwise velocity in defect coordinates and Reynolds shear stress profiles for the cases of Bobke et al. (2017) where β=2. The solid lines are for streamwise locations where β is rising, and the dashed lines are for locations where β is decreasing. The profiles clearly do not collapse. Those from the decreasing β region are well above the others, indicating behavior that is more representative of a higher equilibrium β. The effective β, it appears, is not decreasing as rapidly as the actual β.

The effective β was computed for each streamwise location of each case using Eq. (1). The constant a was set to 4 for all cases. Optimization of this value may be helpful in future analysis, but a=4 was useful for the present cases. Figure 1a shows how β_e lags β. Figure 4 shows mean velocity and Reynolds shear stress profiles for the same cases as in Fig. 3, but from locations with matching β_e=2. The collapse of the profiles is not perfect, but is clearly better than in Fig. 3.

To consider the agreement of profiles at all β in a single plot, Figs. 5a and 5b show the value of the defect velocity and the Reynolds shear stress at y/δ=0.5 for each case as a function of the local β. The location y/δ=0.5 was chosen as representative of the behavior in the center of the boundary layer. Conclusions would be similar if a different y/δ location were chosen. Figures 5c and 5d shows the same quantities as a function of the local β_e. The collapse is improved when matching β_e in regions of both rising and falling β.

The cases of Gungor et al. (2016, 2022, 2024) are considered next. Figure 6 shows G as a function of β. As in Fig. 2, G is initially below the equilibrium curve but then rises well above it while β is still rising. Figure 7 shows profile values at y/δ=0.5 in the format of Fig. 5. As in Fig. 5, the profiles do not agree when β is matched. Matching β_e does result in better agreement between the profiles of cases 1 and 2, but case 3, which includes a dropping β region does not agree. In all cases the values in Fig. 7 are greater than those of Fig. 5 at the same β_e.

The G values for the cases of Volino and Schultz (2026) are shown in Fig. 8. In contrast to Figs. 2 and 6, most of the cases in Fig. 8 lie close to the equilibrium curve. Exceptions are visible in cases 1 and 6 which had a rapid rise of β, resulting in a lag in the rise of G. Cases 14 and 15 had a dropping β as the flow transitioned from an APG to a ZPG. This resulted in G above the equilibrium curve, similar to the

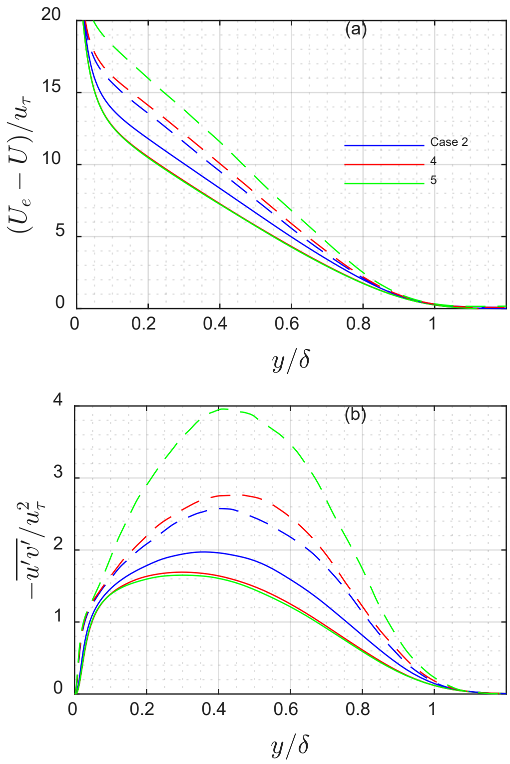

Figure 3. Profiles at locations where β=2 for cases of Bobke et al. (2017): a) Mean velocity in defect coordinates, b) Reynolds shear stress. Solid lines for locations where β is rising, dashed for falling β.

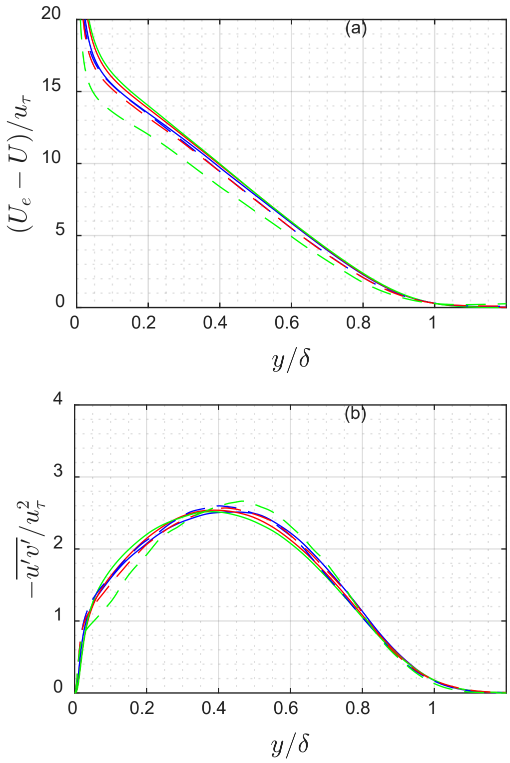

Figure 4. Profiles at locations where β_e=2 for cases of Bobke et al. (2017): a) Mean velocity in defect coordinates, b) Reynolds shear stress. Solid lines for locations where β is rising, dashed for falling β.

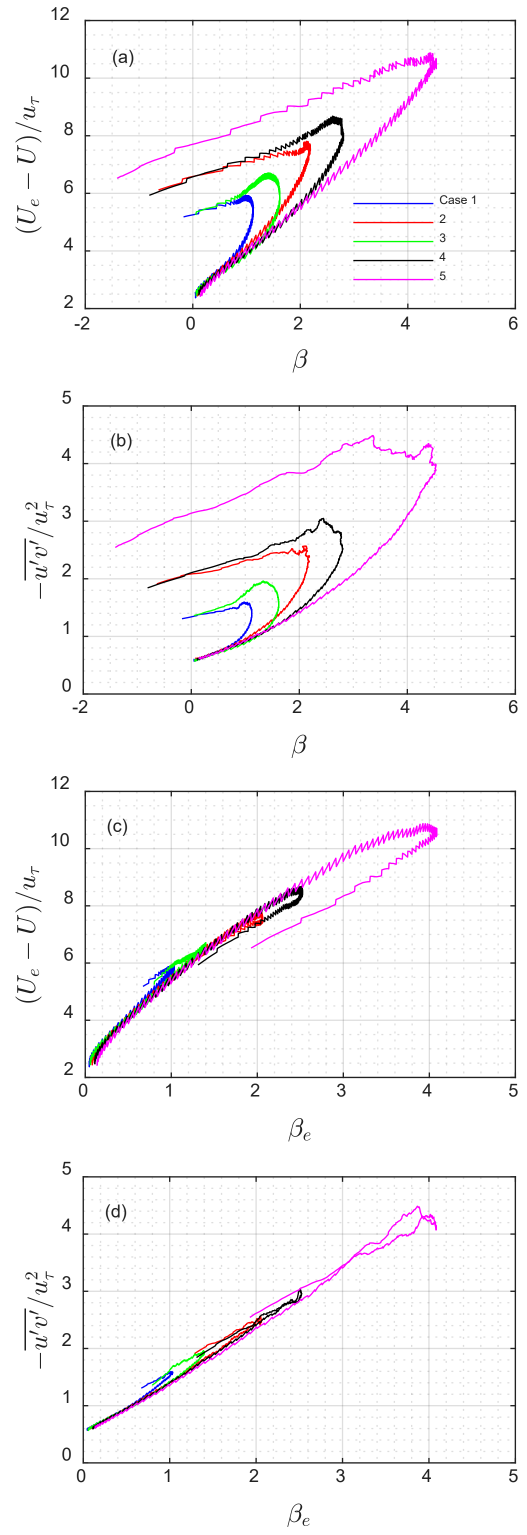

Figure 5. Profiles values at locations where y/δ=0.5 for cases of Bobke et al. (2017): a) Mean velocity in defect coordinates as function of β, b) Reynolds shear stress as function of β, c) Mean velocity in defect coordinates as function of β_e, d) Reynolds shear stress as function of β_e.

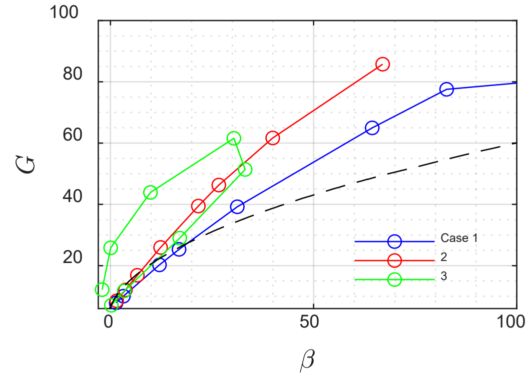

Figure 6. Clauser shape factor as a function of β for cases of Gungor et al. (2016, 2022, 2024). Dashed line is Mellor & Gibson (1966) equilibrium.

cases with dropping β in Fig. 2. The defect velocity and Reynolds stress values at y/δ=0.5 are shown in Fig. 9 in the format of Figs. 5 and 7. The use of β_e improves the collapse somewhat, but the change is not as obvious as in Fig. 5 since the departure from equilibrium was lower for these cases. Improvement is clear in the region where β dropped to zero in cases 14 and 15. At the same β_e, the profile values in Figs. 9c and 9d are approximately the same as those in Figs. 5c and 5d.

CONCLUSIONS

An effective local pressure gradient parameter has been proposed based on an assumption of exponential decay toward the local Clauser pressure gradient parameter at each streamwise location. Results for the data of Bobke et al. (2017) show a collapse of mean velocity and Reynolds stress profiles in nonequilibrium boundary layers when this parameter is matched that is better than the collapse when β is matched. The method was effective in regions of both rising and falling β. Similar results were obtained with the rough and smooth wall data of Volino and Schultz (2026). When applied to the data of Gungor et al. (2016, 2022, 2024), however, the collapse was not as good, and the results did not match those of the other studies. This difference may have been due to the stronger pressure gradients in the Gungor et al. (2016, 2022, 2024) studies and the larger departure from equilibrium in those cases. The new method shows some promise in explaining history effects and collapsing results, but it appears to have limitations. More testing is needed and modifications may be needed, particularly for cases with strong pressure gradients.

DISCLAIMER

The views expressed in this article are those of the authors and do not reflect the official policy or position of the U.S. Naval Academy, the Department of the Navy, the Department of War or the U.S. Government.

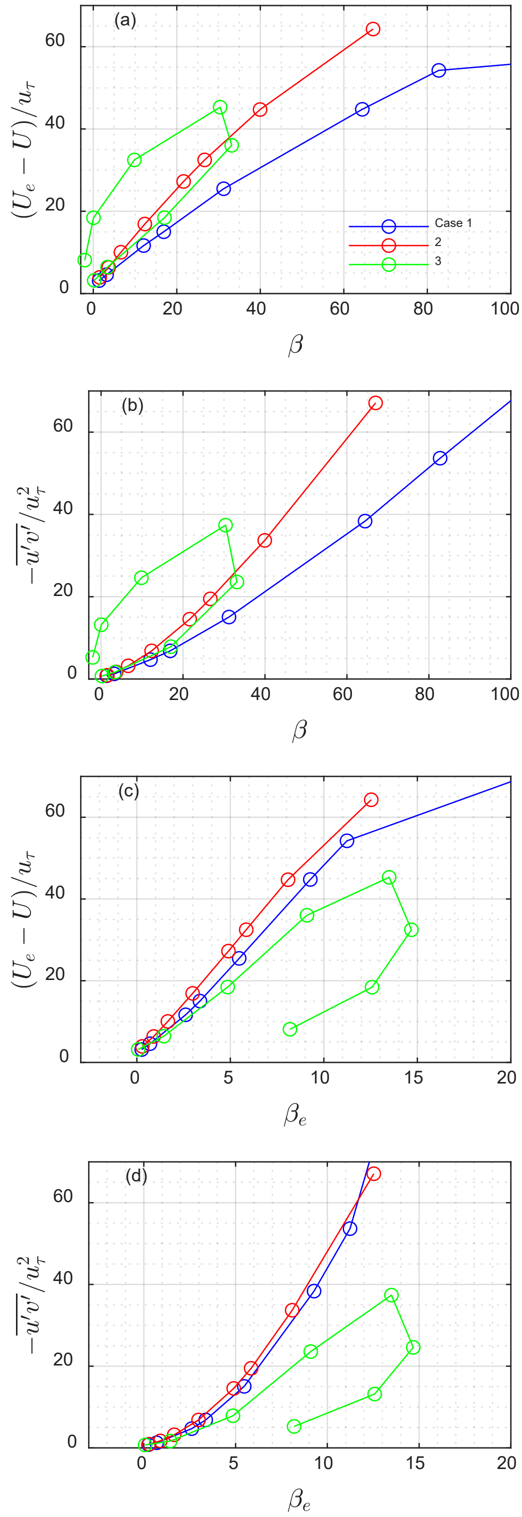

Figure 7. Profiles values at locations where y/δ=0.5 for cases of Gungor et al. (2016, 2022, 2024): a) Mean velocity in defect coordinates as function of β, b) Reynolds shear stress as function of β, c) Mean velocity in defect coordinates as function of β_e, d) Reynolds shear stress as function of β_e.

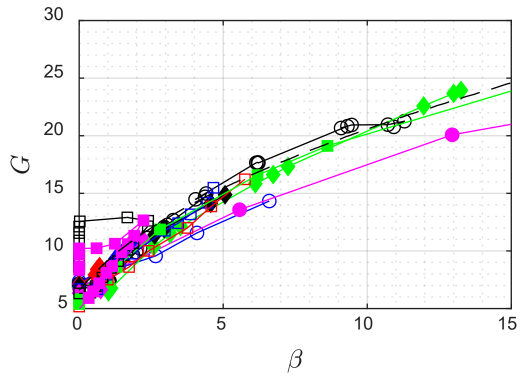

Figure 8. Clauser shape factor as a function of β for cases of Volino and Schultz (2026). Dashed line is Mellor & Gibson (1966) equilibrium.

REFERENCES

Bobke, A., Vinuesa, R., Orlu, R., and Schlatter, P., 2017, “History effects and near equilibrium in adverse-pressure-gradient turbulent boundary layers”, *Journal of Fluid Mechanics*, Vol. 820, pp. 667-692.

Devenport, W. J., and Lowe, K. T., 2022, “Equilibrium and non-equilibrium turbulent boundary layers”, *Progress in Aerospace Science*, Vol. 131, 100807.

Gomez, S. R., and McKeon, B. J., 2025, “Linear analysis characterizes pressure gradient history effects in turbulent boundary layers”, *Journal of Fluid Mechanics*, Vol. 1002, A20.

Gungor, A. G., Maciel, Y., Simens, M. P., and Soria, J., 2016, “Scaling and statistics of large-defect adverse pressure gradient turbulent boundary layers”, *International Journal of Heat and Fluid Flow*, Vol. 59, pp. 109-124.

Gungor, T. R., Gungor, A. G., and Maciel, Y., 2024, “Turbulent boundary layer response to uniform changes of the pressure force distribution”, *Journal of Fluid Mechanics*, Vol. 997, A75.

Gungor, T. R., Maciel, Y., and Gungor, A. G., 2022, “Energy transfer mechanisms in adverse pressure gradient turbulent boundary layers: production and inter-component redistribution”, *Journal of Fluid Mechanics*, Vol. 948, A5.

Maciel, Y., Wei, T., Gungor, A., and Simens, M., 2018, “Outer scales and parameters of adverse-pressure-gradient turbulent boundary layers”, *Journal of Fluid Mechanics*, Vol. 844, pp. 3-35.

Mahajan, A., Deshpande, R., Gungor, T. R., Maciel, Y., and Vinuesa, R., 2026, “Upstream history quantification and scale-decomposed energy analysis for weak-to-strong adverse-pressure-gradient turbulent boundary layers”, *International Journal of Heat and Fluid Flow*, Vol. 117, 110004.

Mellor, G. L., and Gibson, D. M., 1966, “Equilibrium turbulent boundary layers”, *Journal of Fluid Mechanics*, Vol. 24, pp. 225-253.

Preskett, T., Virgilio, M., Jaiswal, P., and Ganapathisubramani, B., 2025, “Effects of pressure-gradient histories on skin friction and mean flow of high Reynolds number turbulent boundary layers over smooth and rough walls”, *Journal of Fluid Mechanics*, Vol. 1010, A30.

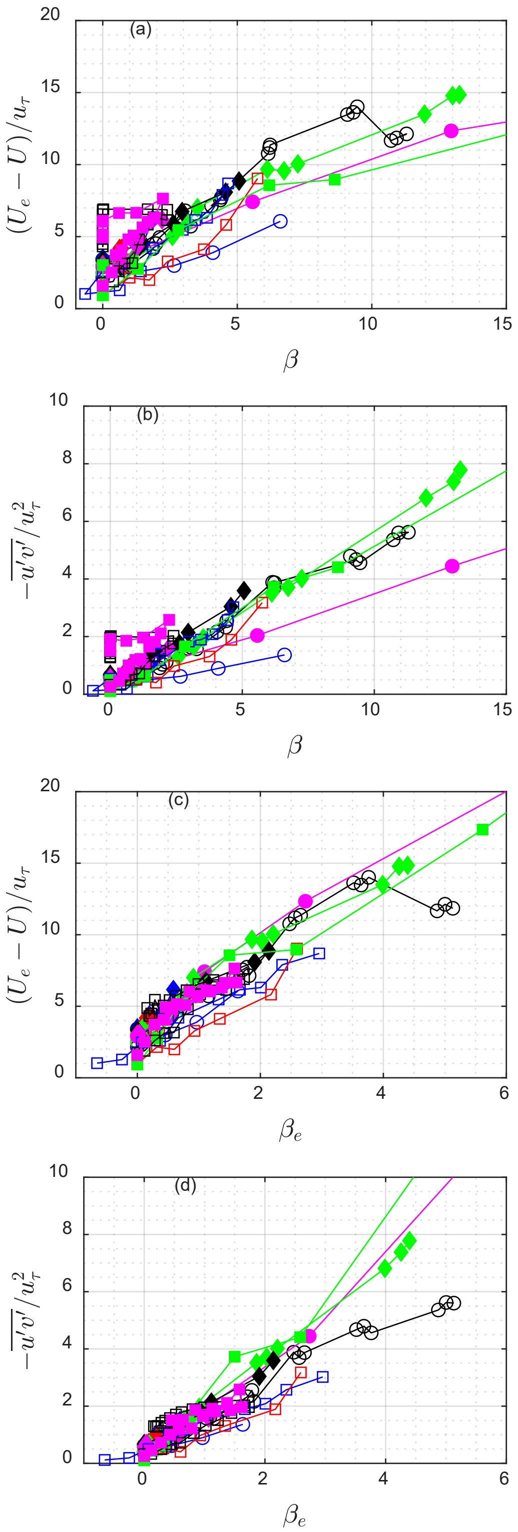

Figure 9. Profiles values at locations where y/δ=0.5 for cases of Volino and Schultz (2026): a) Mean velocity in defect coordinates as function of β, b) Reynolds shear stress as function of β, c) Mean velocity in defect coordinates as function of β_e, d) Reynolds shear stress as function of β_e.

Vinuesa, R., Orlu, R., Sanmiguel, V., Ianiero, C., Discetti, S., and Schlatter, P., 2017, "Revisiting history effects in adverse-pressure-gradient turbulent boundary layers", *Flow Turbulence and Combustion*, Vol. 99, pp. 565-587.

Virgilio, M., Preskett, T., Jaiswal, P., and Ganapathisubramani, B., 2025, "Pressure gradient history effects on integral quantities of turbulent boundary layers: experiments and data-driven models", *Journal of Fluid Mechanics*, Vol. 1014, A2.

Volino, R. J., and Schultz, M. P., 2026, "Response of smooth- and rough-wall boundary layers to non-equilitrbium adverse pressure gradients," *Journal of Fluid Mechanics*, in press, doi:10.1017/jfm.2026.11277.